Title: Bulk and spatially resolved extracellular metabolomics of free-living nitrogen fixation

Author names and affiliations:

Darian N Smercina [a], Young-Mo Kim [a], Mary S Lipton [b], Dusan Velickovic [b], Kirsten S Hofmockel [a, c]

[a] Biological Sciences Division, Earth and Biological Sciences Directorate, Pacific Northwest National Laboratory, Richland, WA, USA

[b] Environmental Molecular Sciences Laboratory, Pacific Northwest National Laboratory, Richland, WA 99354, USA

[c] Department of Agronomy, Iowa State University, Ames, IA 50010

Corresponding author: Darian Smercina, Battelle for the US DOE, 3335 Innovation Blvd., Richland, WA 99354, (509) 375-2950, darian.smercina@pnnl.gov

ORCID IDs:

Darian Smercina: 0000-0002-8484-3827

Young-Mo Kim: 0000-0002-8972-7593

Mary Lipton: 0000-0001-7749-0077

Dusan Velickovic: 0000-0001-7945-9620

Kirsten Hofmockel: 0000-0003-1586-2167

Keywords: Soil microbial ecology, multi-scale, spatially resolved, nitrogen fixation, microbial metabolomics, GC-MS, MALDI MSI

Competing interests: The authors declare no conflicts of interest.

Funding: D.N.S. is also grateful for the support of the Linus Pauling Distinguished Postdoctoral Fellowship program through Pacific Northwest National Laboratory. Pacific Northwest National Laboratory is a multiprogram national laboratory operated by Battelle for the U.S. Department of Energy under contract DE-AC05-76RL01830. This research was performed using resources at the Environmental Molecular Sciences Laboratory (EMSL; grid.436923.9), a DOE Office of Science User Facility sponsored by the Biological and Environmental Research program.

Abstract

Soil microorganisms drive ecosystem function, but challenges of scale between microbe and ecosystem hinder our ability to accurately quantify and predictively model the soil microbe-ecosystem function relationship. Quantifying this relationship necessitates studies that systematically characterize multi-omics of soil microorganisms and their activity across sampling scales from spatially resolved to bulk measures, and structural complexity, from liquid pure culture to *in situ*. To address this need, we cultured two diazotrophic bacteria in liquid and solid media, with and without nitrogen (N) to quantify differences in extracellular metabolites associated with nitrogen fixation under increasing environmental structural complexity. We also quantified extracellular metabolites across sampling scales including bulk sampling via GC-MS analysis and spatially resolved analysis via MALDI mass spectrometry imaging. We found extracellular production of inorganic and organic N during free-living nitrogen fixation activity, highlighting a key mechanism of terrestrial N contributions from this process. Additionally, our results emphasize the need to consider the structural complexity of the environment and spatial scale when quantifying microbial activity. We found differences in metabolite profiles between culture conditions, supporting previous work indicating environmental structure influences microbial function, and across scales, underscoring the need to quantify microbial scale conditions to accurately interpret microbial function.

Importance: Studying soil microorganisms, both who is present and what they are doing, is a challenge because of vast differences in scale between microorganism and ecosystem and because of inherent complexities of the soil system (e.g., opacity, chemical complexity). This makes measuring and predicting important ecosystem processes driven by soil microorganisms,

like free-living nitrogen fixation, difficult. Free-living nitrogen fixing bacteria play a key role in terrestrial nitrogen contributions and may represent a significant, yet overlooked, nitrogen source in agricultural systems like bioenergy crops. However, we still know very little about how free-living nitrogen fixation contributes nitrogen to terrestrial systems. Our work provides key insight by hierarchically increasing structural complexity (liquid vs. solid culture) and scale (spatially resolved vs. bulk) to address the impact of environmental structure and sampling scale on detection of free-living nitrogen fixation and to identify the forms of nitrogen contributed to terrestrial systems by free-living nitrogen bacteria.

Introduction

Soil microorganisms are a key link between above and belowground ecosystem function, driving energy and nutrient transfer between the atmosphere, biosphere, and pedosphere (1-3). Multi-omic analysis aimed at understanding the structure and function of these microorganisms has become a routine tool for environmental samples. Despite generating large amounts of data, even quantitatively linking 'omics of a specific function (e.g. functional genes and proteins) to measures of that function is often unsuccessful (2-6) because of inherent challenges of studying soils (5-7) and soil microorganisms. Given these challenges, the importance of linking microbial community structure to function has been questioned (8, 9), however without clearer understanding of how microorganisms relate to observed functions we cannot yet rule out the importance of individual microbial community members. Our limited ability to quantitively link soil microbial communities to ecosystem function hinders our understanding of ecosystem processes, leaving us vulnerable to losing vital ecosystem services provided by our soils, particularly in the face of climate change (10).

Quantifying the link between soil microorganisms and ecosystem function requires systematic studies that characterize multi-omics of soil microorganisms and their functions hierarchically across scales of space and complexity (Fig. 1; (4, 11). *In vitro* studies using pure cultures or limited species are an appealing option and have the potential to provide fundamental microbial and ecological knowledge (10, 12, 13). However, culturing conditions are often quite different from those experienced by microorganisms in soil and attachment to surfaces has been shown to impact microbial growth and function (14, 15). Thus, physical structure influences microbial function, and it is therefore essential for studies to systematically characterize multi-omics and function *in vitro* under growth conditions of increasing complexity (e.g. environmental structure) in order to determine how culture work may better inform *in situ* processes (Fig. 1).

In this study, we explored two questions surrounding the microbe-ecosystem function relationship: (1) Are there microbial metabolomic signatures associated with target ecosystem processes? (2) How do growth conditions and sampling scale influence metabolomic signatures? We used free-living nitrogen fixation (FLNF), biological nitrogen fixation (BNF) carried out by heterotrophic bacteria (diazotrophs), as a model microbial process and ecosystem function to address these questions. FLNF is carried out by a wide diversity of soil bacteria and occurs in all terrestrial biomes, contributing significantly to terrestrial N (16, 17). These contributions are thought to occur predominately through release of ammonium and organic N sources, like amino acids, as occurs during symbiotic BNF (18-21). Thus, extracellular metabolites may be valuable to understanding FLNF and identifying biosignatures.

We examined extracellular metabolites from two diazotrophic bacteria cultured under conditions that promote (N-free) or inhibit (N-rich) FLNF. Additionally, cultures were grown in

liquid or on solid media to examine the impact of physical structure on detected metabolites. Lastly, we examined extracellular metabolites across sampling scale from spatially resolved measures using matrix-assisted laser desorption/ionization mass spectrometry imaging (MALDI–MSI) to bulk sampling via gas chromatography–mass spectrometry (GC-MS) analysis. We hypothesized: (1) bulk metabolite profiles differ between N-rich and N-free conditions and also between liquid and solid cultures, (2) there are extracellular metabolites associated with FLNF activity and only observed under N-free conditions, (3) these extracellular metabolites are detectable with bulk and spatially resolved sampling, and (4) N-containing compounds are produced during FLNF and are readily detectable in bulk and spatially resolved extracellular metabolites under N-free conditions.

Results

Microbial biomass – total biomass, biomass C, and biomass N

Total microbial biomass, including cells and associated debris such as EPS, was collected from all treatments except for the AV N-rich solid treatment. In this case, microbial colonies had grown into and below the agar surface and it was not possible to collect biomass. Total biomass was highly variable across all treatments (CV across treatments ranged from 4.6% to 100.4%) and there were no significant differences observed with N treatment, culture type, or organism (Fig. 2D). Both biomass C and N differed significantly across treatments (Fig. 2A and 2B, respectively). In general, C and N content were greater in N-rich treatments where N was readily available compared to N-free treatments. There was also a trend towards greater biomass C and N from solid media, but this was mostly observed in the N-rich treatments. These C and N values translated to C:N ratios that predominately differed only between N treatments with the N-free

138 treatment resulting in greater biomass C:N ratios than N-rich conditions, regardless of culture
139 type or organism (Fig. 2C).
140
141 *Extracellular ammonium availability*
142 Extracellular ammonium availability was measured supernatant and rinsate samples and
143 was detected in all treatments regardless of culture type, N treatment, or organism. On a per unit
144 biomass basis, ammonium concentrations differed significantly by organism ($F = 16.390$, $p = 0.0012$) and by the interaction between culture type and N treatment ($F = 35.411$, $p < 0.0001$).
145
146 Extracellular ammonium availability per unit biomass was over 8x greater in PP than AV
147 cultures (Fig. 3A). Under N-free conditions, ammonium availability was greater in liquid than in
148 solid culture while in N-rich conditions the opposite was observed (Fig. 3B). Extracellular
149 ammonium availability is of particular interest in N-free treatments as ammonium is
150 hypothesized to be released from cells actively fixing N and thus represents a major form of N
151 contributed by FLNF to terrestrial systems (18, 33). Therefore, we also calculated the percent of
152 fixed N available as extracellular ammonium (Fig. 4). Total fixed N was estimated as total
153 biomass N measured in N-free treatment samples. We find only upwards of 7.5% (± 2.3) of fixed
154 N is readily available as extracellular ammonium. This did not differ significantly between
155 culture types ($F = 2.171$, $p = 0.184$), though ammonium concentrations in solid culture tended to
156 be lower than those in liquid culture.
157
158 *Bulk extracellular metabolites*
159 Across all treatments, 307 metabolites were detected with bulk sampling and of these 93
160 were successfully annotated (>80% confidence). The total number of detected metabolites

differed between treatment groups (Supp. Fig. 2) with generally more metabolites detected in N-free treatments, the majority of which were within the unannotated portion of detected metabolites. Distinct metabolite profiles, represented by Bray-Curtis and Jaccard distance based on all detected metabolites, were observed between N treatment, culture type, and their interaction (Fig. 5; Table 1). N treatment and culture type, together with their interaction, explain over 50% of the variance in metabolite profiles based on peak intensity (Fig. 5A) and based on presence-absence (Fig. 5B). Metabolite profiles based on abundance separated predominantly by culture type and then by N treatment (Fig. 5A). Metabolite profiles based on presence-absence show clear separation between culture types for N-rich treatments but have little separation under N-free conditions (Fig. 5B).

Because FLNF activity is hypothesized to result in the release of N-containing metabolites (33), we focused on N-containing extracellular metabolites. Of the 93 annotated metabolites detected through bulk sampling, 35 were N-containing. We found significant differences in N-containing compounds across treatments, after correcting for background metabolites, with significant interactions between N treatment, culture type, and organism ($F = 10.695$, $p = 0.0048$). N-free treatments were richer in N-containing metabolites (Supp. Fig. 3) but had similar or significantly lower total abundances of N-containing metabolites compared to N-rich treatments (Fig. 6). Examining the specific composition of these N-containing compounds, we found a variety of amino acids in N-free samples not well represented in N-rich samples (Supp. Fig. 3), but only a few N-containing metabolites were unique to N-free conditions including pantothenic acid, L-pyroglutamic acid, L-glutamic acid, and 4-pyridoxic acid.

Spatially resolved extracellular metabolites

Across all treatments, METASPACE analysis identified 69 metabolites in spatially resolved samples of which 41 were N-containing. However, only a few potential amino acids were detected at this resolved microbial scale including L-leucine and L-valine. These were only at detectable concentrations within the N-rich treatment (Fig. 7) unlike the diversity of amino acids detected in bulk samples predominately in association with N-free treatments. Observationally, N-free treatments seemed to be characterized by unique presence of organic acids rather than N-containing compounds. However, we did identify a few N-containing compounds unique to N-free treatments at the microbial scale including inosine and 4-pydroxic acid (Fig. 7). Inosine was detected in N-free treatments of both AV and PP and was not at detectable levels in N-rich treatments. Also, much like bulk sampling scale detection, 4-pyridoxic acid was exclusively detected in AV N-free treatment samples.

Discussion

We explored the impact of N availability and physical structure on the extracellular metabolomics of diazotrophic bacteria across sampling scales from the spatially resolved to bulk. We find evidence of extracellular organic and inorganic N contributions from FLNF underscoring a key mechanism of terrestrial N contributions from FLNF. In general, we find physical structure and microbial function (e.g. FLNF) alter extracellular metabolite profiles and influence the detection of metabolites at bulk and spatially resolved scales.

Nitrogen contributions from FLNF

Products of BNF by symbiotic diazotrophs are well-studied and typically observed as ammonia and ammonium with contested evidence for production of amino acids (18-21). This

knowledge of symbiotic BNF is thought to translate directly to FLNF leading to the assumption that free-living diazotrophs also excrete ammonia/ammonium into the surrounding environment during BNF. However, ammonia produced during FLNF is rapidly assimilated through conversion to glutamine or glutamate via the glutamine synthetase (GS) and glutamate synthetase (GOGAT) pathways (34). Thus, excreted ammonium would necessarily be in excess of these assimilation pathways (34). Ammonium excretion has been observed in wild-type *Azotobacter vinelandii* DJ, at concentrations between ~2 and ~25 μM (35, 36), values within range of those measured in this study (Supp. Fig. 4). However, in many cases measurable ammonium excretion was only observed from *Azotobacter vinelandii* cultures genetically altered to disrupt the GS-GOGAT pathways or facilitate constitutive nitrogenase synthesis (37-40).

An alternative hypothesis to ammonium excretion is that N contributions occur as organic N, either through direct release of N-rich compounds like amino acids (18, 21) or through turnover of dead biomass (41). Our bulk metabolomics data support this hypothesis with many N-containing organic compounds, including amino acids detected in N-free treatments. In fact, N-free treatments were richer in N-containing compounds than N-rich conditions, particularly when comparing against N-rich solid media which had few N-containing metabolites (Supp. Fig. 3). The structure of our study did not allow us to determine whether these organic molecules were directly excreted by active, N-fixing cells or released during cell turnover. However, other metabolites detected in the system suggest cell turnover contributed at least partially to this N release. For example, we detected inosine in both bulk and spatially resolved analysis, and it was unique to N-free treatments in spatially resolved samples. Inosine, a metabolic product of adenine degradation likely indicates salvage activities by the bacterial populations (42, 43) and could indicate freely available nucleotides from cell lysis and turnover. FLNF may therefore

229 contribute available N through increasing microbial biomass and turnover, but this needs to be
230 verified in future studies. Regardless of whether these N-containing compounds are actively
231 excreted or released after cell death, this metabolic exchange with the surrounding environment
232 highlights a key mechanisms of terrestrial N contributions from FLNF.
233
234 *In vitro vs in situ analysis – identification of biosignatures*
235 Through bulk and spatially resolved analysis, we found few N-containing metabolites
236 exclusive to N-free treatments. At bulk scale, these include pantothenic acid, L-pyroglutamic
237 acid, L-glutamic acid, and 4-pyridoxic acid. We similarly find 4-pyridoxic acid at the spatially
238 resolved microbial scale as well as nine other metabolites including inosine. 4-pyridoxic acid
239 was unique to AV N-free treatments at the microbial scale. However, despite being uniquely
240 associated with N-free treatments and therefore microbial populations actively fixing N, it may
241 be difficult to assign these as a signature of FLNF function. Of these compounds, only L-
242 glutamic acid has a direct association with the FLNF pathway. Other metabolites seem more
243 indicative of microbial nutrient needs and function. For example, pantothenic acid, vitamin B_5, is
244 involved in the synthesis of coenzyme A and is a coenzyme for many reactions involved in
245 protein and lipid metabolism (44-46). This is particularly important for the processing of organic
246 acids like malate, the main C source provided in this study. Thus, the detection of vitamin B_5 is
247 likely indicative of malate metabolism via the TCA cycle and its unique detection in the N-free
248 treatment suggests a higher respiration rate in these N-fixing populations than in the N-rich
249 populations. Increased respiration is a common response among diazotrophs in oxygenated
250 environments as a protection mechanism to prevent or reduce denaturation of nitrogenase via
251 oxygen (17, 47, 48). We also identified 4-pyridoxic acid, a derivative of pyridoxine (vitamin B_6).

Pyridoxine is a key cofactor in amino acid, fatty acid, and carbohydrate metabolisms, but can also act an oxygen protectant (46). During this redox reaction, pyridoxine degrades and can result in 4-pyridoxic acid. *A. vinelandii* has been observed to produce B vitamins while under diazotrophic conditions and this seems to be a hallmark of FLNF for this organism (46, 49, 50). Though not directly associated with the N-fixation pathway, these vitamins may tangentially indicate bacteria functions surrounding FLNF such as oxygen regulation and highlight the need to analyze bacterial function holistically rather than focusing on single reactions or pathways.

Additionally, the limited number of unique extracellular metabolites detected in N-free treatments suggests some microbial functions may not have detectable or unique biosignatures, in the form of extracellular metabolites. This is an important consideration when applying metabolomics to the study of complex soil systems. Soil metabolomics are increasingly being used to study soil microbial ecology and biogeochemical function and have been successfully applied to soil carbon cycling (51-54). However, metabolites are by definition the by-products of and substrates for metabolic function, and turnover rapidly in soils (55, 56). Therefore, typical soil extractions to collect extracellular components (e.g. K_2SO_4 extracts, leachate; (57, 58) only capture what is not consumed by the microbial community. This includes metabolites available in dissolved organic matter pools at the time of sampling and metabolites readily exchangeable from mineral surfaces (59). In both cases, metabolites could be temporally separated from their originating processes making it difficult to trace back the associated metabolic pathway. It could be even more challenging to capture metabolic biosignatures from nutrient-limited communities, such as those in bulk soil. Under nutrient-limited conditions, resulting metabolic products are likely to be rapidly assimilated or, in the case of processes like FLNF, not released to the surrounding environment. The potential signature compounds of FLNF found here (e.g. amino

acids and B-vitamins) are also not uniquely produced by FLNF processes and would be difficult to directly link to FLNF *in situ*. We acknowledge our study system may provide a biased view on this issue, being a closed incubation system unlike soils where metabolites may diffuse away from microbes and persist in the environment. However, these findings highlight a key need to understand the soil microhabitat (11).

Lastly, our work highlights the importance of considering culture conditions and their association to *in situ* conditions as we observed clear differences in metabolite profiles between liquid and solid culture. Interestingly, though culture type strongly influenced metabolite profiles, it played a secondary role to N treatment in influencing the number of detected metabolites. This was particularly notable when N was readily available, where presence-absence based profiles were distinct between liquid and solid culture, but only under N-rich conditions. These differences in metabolite profiles were likely not driven by differences in biomass production as culture type had small and non-significant impacts on microbial metrics, like total biomass, and biomass C and N content. Thus, these responses seem specifically associated with the presence or absence of physical structure in the environment. Additionally, these findings suggest nutrient limitation, as experienced in the N-free treatments, may be a stronger driver of microbial activity than physical structure and simplified liquid culture may be somewhat informative to nutrient-limited *in situ* conditions.

Implications scaling from microbial scale to bulk sampling

The combination of techniques in this study allowed us to explore detection of metabolites across scales from spatially resolved, relevant to microorganisms, to bulk, relevant for soil microbial ecology analysis. MALDI MSI allowed us to resolve abundances of

298 extracellular metabolites on solid media at a microbial scale. Using GC-MS, we were able to
299 evaluate detection of extracellular metabolites at the bulk scale. While the detection ranges of
300 these two techniques do not fully overlap (50 – 500 m/z for GC-MS and 92 – 700 m/z for
301 MALDI), many metabolites of interest to this study are measurable with both techniques
302 providing valuable information about metabolite detection and sampling scale. It is also
303 important to note that a lack of detection is not equivalent to metabolite absence but only
304 indicates metabolite concentrations were below detection.

305 Through bulk sampling, we found a wide variety of N-containing compounds in N-free
306 samples, but generally lower abundances of N-containing compounds than in the N-rich
307 treatment. While N-containing compounds are characteristic of N-free samples at a bulk scale,
308 these treatments had fewer N-containing metabolites when spatially resolved at the microbial
309 scale. Interestingly, there was a shift in amino acid detection between spatially resolved and bulk
310 scales where amino acids were commonly detected in N-free samples at bulk scale, but in N-rich
311 samples when spatially resolved. This somewhat counterintuitive result highlights differences in
312 N competition at the microbial scale and its influence on bulk measurements.

313 First, detection of a diverse array of amino acids in the N-free treatment in bulk sample,
314 but not in spatially resolved samples suggests N competition at the microbial scale resulted in
315 rapid uptake of amino acids, while extraction of the bulk metabolite pool likely captured the
316 cumulative low abundance signal of the entire system. Amino acids are shown to have short
317 residence times in soils and experience rapid uptake and turnover (60, 61). In the case of
318 microbial vs. bulk scale, it is likely the spatially resolved pool of extracellular amino acids
319 collected from microbial colonies (~200 μm spatial resolution) was small and often below
320 detection. However, in bulk sampling of millions of cells, a larger pool of amino acids coupled to

our sampling method could have allowed amino acids to diffuse away and accumulate to detectable levels.

Second, biofilm formation is likely to influence diffusion of metabolites into the surrounding environment (62, 63). Bacteria tend to live in biofilms in their natural environments rather than as individually dispersed cells (64). However, the impact of surrounding environmental conditions, including nutrient availability, on biofilm production is unclear. For example, some studies suggest nutrient limiting conditions may promote greater biofilm formation (65), while others suggest biofilm formation is greater under more favorable growth conditions (66, 67). This is particularly notable for diazotrophs as biofilms can play a role in oxygen protection (47), thus investment in biofilm could be beneficial to FLNF activity. Yet, under severe N limitation imposed by an N-free environment the high energy demands of FLNF may limit investment in biofilm. While not directly measured in this study, we noted solid agar plates of *Azotobacter vinelandii* and *Paenibacillus polymyxa* cultures had visually greater biofilm production under N-rich than N-free conditions. Thus, diffusion of amino acids away from populations would have been more easily achieved in the N-free treatment. This is evidenced by the similarity between metabolite chemistry in liquid and solid culture under N-free treatments (Fig. 5B). Similarly, a small number of amino acids were detected in spatially resolved samples from N-rich treatments, but not in bulk samples for the similar N-rich solid media treatment. This could have resulted from greater biofilm formation under N-rich conditions and limited diffusion of small molecules away from cell populations.

The detection of small molecules across scales has important implications for the influence of soil microbial communities on their surrounding environment. In general, our results indicate microbial scale processes drive bulk metabolite availability. The N-rich treatment in this

344 experiment is an optimal environment and most representative of carbon and nutrient rich soil
345 environments like the rhizosphere or detritusphere. Our findings suggest these conditions would
346 result in production of valuable small molecules, like N-rich amino acids, potentially
347 exchangeable with the immediate environment, but biofilm formation may limit diffusion far
348 into the soil environment. Under limiting conditions of the N-free treatment, similar those of
349 bulk soil, microbial activity produces valuable metabolites, like amino acids, but competition
350 between microbes reduces the exchange of these molecules. Understanding how these
351 differences in microbial scale conditions influence microbial activity and detectability of
352 function is crucial to accurately linking microbe and ecosystem.
353
354 **Conclusions**
355 We demonstrate extracellular production of inorganic and organic N during FLNF and
356 reveal the importance of habitat conditions and sampling scale when quantifying microbial
357 activity. Across bulk and spatially resolved sampling scales, we identified metabolites uniquely
358 associated with FLNF activity including several B-vitamins, which may play roles in mitigating
359 oxygen damage to nitrogenase. Despite finding unique metabolites and potential biosignatures,
360 many detected metabolites are not exclusively produced through FLNF related pathways, thus
361 would be difficult to assign to FLNF for *in situ* soil samples. This would likely hold true for
362 other processes under nutrient limited conditions where metabolic products are rapidly
363 assimilated and not captured during sampling. Our findings highlight the need to carefully
364 consider both structural complexity and sampling scale when quantifying microbial function. We
365 found culture conditions to be a key driver of metabolite chemistry under N-rich and N-free
366 conditions, indicating physical structure influences microbial processes. Across scales, our

results indicate high N competition at the microbial scale under N-free conditions, while at the bulk scale N appeared readily available within the microbial environment. These differences in environmental conditions across scales could lead to incorrect interpretations of microbial function as immediate conditions surrounding microorganisms will drive their activity and may not necessarily match what is measured through bulk or composite sampling.

Materials and Methods

Culture conditions

Two diazotrophic bacteria with distinct growth strategies (e.g. gram-negative vs gram-positive) and fully sequenced genomes (22, 23)were chosen for this study, *Azotobacter vinelandii* DJ (ATCC BAA 1303; hereafter AV) and *Paenibacillus polymyxa* (ATCC 842; hereafter PP). Bacteria were cultured under N-free and N-rich conditions, respectively promoting or inhibiting FLNF. Nfb media, commonly used to isolate diazotrophs (24), was used for N-free treatments, and was supplemented with tryptone for N-rich treatments. Both treatments contained 1.79 g C L^{-1} as malic acid and N-rich media contained ~1.33 g N L^{-1} as tryptone. Cultures were grown in liquid or solid agar media and all media was autoclave sterilized prior to inoculation.

Thirty samples were cultured (2 organisms x 2 N treatments x 2 media types x 3 replicates, plus controls) for bulk analysis with an additional set of 14 samples (2 organisms x 2 N treatments x 3 replicates, plus controls) on solid media for spatially resolved analysis. Cultures were grown in a temperature-controlled incubator at 25˚C to 10^7 CFU mL^{-1}, based on liquid cultures, and then harvested for analysis of extracellular metabolites at two scales – bulk sampling via MPLEx extraction and GC-MS (25) and spatially-resolved sampling via colony

analysis with MALDI MSI. Extracellular ammonium availability and microbial biomass, including total biomass, biomass carbon (C) and biomass N, were also measured. Because FLNF activity is necessary for microbial growth under N-free conditions, measures of total biomass and biomass N are used as estimates of FLNF (24).

Sample collection

Extracellular metabolites were collected from liquid culture by centrifuging culture tubes to pellet cells and collecting the resulting supernatant for bulk analysis as described below. Cell pellets were resuspended in autoclave sterilized nanopure water, immediately flash frozen on liquid nitrogen, and stored at -80˚C until further analysis. Extracellular metabolites were collected from solid media for bulk and spatially resolved analysis. Bulk samples were collected by washing culture plate surfaces with autoclave sterilized nanopure water and collecting the resulting rinsate. Samples were collected for spatially resolved analysis as described below. Lastly, microbial colonies from rinsate plates were collected from the surface by gentle scraping, transferred to autoclave sterilized nanopure water, flash frozen on liquid nitrogen, and stored at -80˚C until further processing.

Microbial biomass – total biomass, biomass C, and biomass N

Frozen cell pellets and colonies were lyophilized until completely dry and weighed to obtain total biomass, including cells and associated debris such as exopolysaccharides (EPS). Dried biomass was ground using sterile steel beads and then analyzed for C and N content on a VarioTOC Cube (Elementar, Langenselbold, Germany).

Extracellular ammonium availability

We measured extracellular ammonium concentrations in supernatant and rinsate samples using a high-throughput colorimetric ammonium assay (26). Briefly, samples were pipetted in

413 triplicate into clear 96-well plates and incubated with ammonium salicylate and ammonium
414 cyanurate reagents to facilitate color change via the Berthelot reaction. Plates were read for
415 absorbance at 610 nm on a Synergy H1 plate reader (BioTek Instruments, Inc., Winooski, VT,
416 USA).

417 *Bulk metabolomics – GC-MS*

418 Bulk metabolomics analysis was conducted on 1 ml subsamples of undiluted, supernatant
419 and rinsate samples. Supernatant and rinsate samples were prepared for metabolite analysis via
420 GC-MS following the MPLEx protocol for simultaneous metabolite, protein, and lipid extraction
421 (25). Additionally, 1 ml of supernatant and rinsate from sterile liquid culture and solid culture
422 plates were also extracted via MPLEx as background controls. This extraction method allows
423 simultaneously collection of metabolites, lipids, and proteins; however, lipid fractions were not
424 analyzed in this study. Additionally, protein yields were too low for downstream analysis.
425 Metabolite samples were completely dried under speed-vacuum concentrator and chemically
426 derivatized prior to analysis by GC-MS as reported previously (27). The m/z range of derivatized
427 metabolites scanned was 50 – 550 m/z which can detect organic acids, amino acids, and mono to
428 tri-saccharides. Raw GC-MS data were processed using the PNNL in-house metabolomics
429 database, which can identify metabolites using two dimensional matching factors (fragmented
430 spectrum + retention index (28), and with cross-checking against commercially available NIST
431 20/Wiley 11th GC-MS spectral databases (25, 29).

432 *Spatially resolved metabolomics – MALDI MSI*

433 Samples were prepared for spatially resolved analysis via MALDI-MSI using a
434 previously described workflow (30). Briefly, areas of agar were excised from Petri dishes and
435 placed onto double-sided adhesive copper tape adhered to indium tin oxide (ITO)-coated glass

436 slides (Bruker Daltonics; Supp. Fig 1.). This approach enhanced our sensitivity for analysis in
437 negative ionization mode and improved adhesion of agar onto the MALDI target. Samples were
438 dried at room temperature overnight, then treated with MALDI matrix using a HTX TM-Sprayer
439 (HTX Technologies). For analysis in negative-ion mode, 7 mg mL^{-1} of N-(1-naphthyl)
440 ethylenediamine dihydrochloride (NEDC) in 70% MeOH was sprayed with eight passes at 1,200
441 µL min^{-1}, 75°C, a spray spacing of 3 mm, and a spray velocity of 1,200 mm min^{-1}. MALDI-MSI
442 was performed on a 15-Tesla Fourier transform ion cyclotron resonance (FTICR)-MS (Bruker
443 Daltonics, Billerica, MA, USA) equipped with SmartBeam II laser source (355 nm) using 200
444 shots $pixel^{-1}$ with a frequency of 2 kHz and a step size of 200 µm. FTICR-MS was operated to
445 collect m/z 92–700, using a 209-ms transient, which translated to a mass resolution of R ~
446 70,000 at 400 m/z. Metabolites in this range can typically be detected to fmol concentrations.
447 *Data Analysis*
448 A factorial ANOVA with N treatment, culture type, organism and their interactions as
449 main effects followed by a Tukey's post hoc test was used to determine treatment differences for
450 measured variables. Prior to statistical analysis, bulk metabolite values were blank corrected by
451 subtracting peak intensities identified in background controls of the associated treatment.
452 Differences in bulk metabolite chemistry were evaluated using distance matrices based on peak
453 intensities (Bray-Curtis) presence-absence (Jaccard) generated from all detected metabolites
454 using R *vegan* (31). Differences between culture type, N treatment, and organism were
455 determined via PERMANOVA using *adonis* in R *vegan*. Spatially resolved metabolite data was
456 acquired using FlexImaging (v 4.1, Bruker Daltonics), and image processing, segmentation, co-
457 localization analysis and visualization were performed using SCiLS (Bruker Daltonics). The list
458 of m/z values that colocalized with the colonies were uploaded to the METLIN

(https://metlin.scripps.edu) for putative molecular annotations based only on accurate m/z, secured by using a 3-ppm window during the search. imzML files (created by SCiLS) of our analyses were also uploaded to METASPACE (32) for metabolite annotation based on both accurate m/z and a comprehensive bioinformatics framework that considers the relative intensities and spatial colocalization of isotopic peaks as well as quantifies spatial information with a measure of spatial chaos followed by the estimation of the False Discovery Rate. For this purpose, we used KEGG-v1 and NPA-2019-08 (Natural Product Atlas) databases that are available in METASPACE. METASPACE uses by default 3 ppm window in its annotation engine.

Acknowledgements: We would like to thank Heather Olson, Carrie Nicora, and Jesse Trejo for sampling processing work and for taking time to carefully train D.N.S. on the methods. D.N.S. is also grateful for the support of the Linus Pauling Distinguished Postdoctoral Fellowship program through Pacific Northwest National Laboratory. Pacific Northwest National Laboratory is a multiprogram national laboratory operated by Battelle for the U.S. Department of Energy under contract DE-AC05-76RL01830. This research was performed using resources at the Environmental Molecular Sciences Laboratory (EMSL; grid.436923.9), a DOE Office of Science User Facility sponsored by the Biological and Environmental Research program.

References

1. Falkowski PG, Fenchel T, Delong EF. The microbial engines that drive Earth's biogeochemical cycles. science. 2008;320(5879):1034-9.

2. Hall EK, Bernhardt ES, Bier RL, Bradford MA, Boot CM, Cotner JB, et al. Understanding how microbiomes influence the systems they inhabit. Nature microbiology. 2018;3(9):977-82.

3. Jansson JK, Hofmockel KS. The soil microbiome—from metagenomics to metaphenomics. Current opinion in microbiology. 2018;43:162-8.

4. Graham EB, Knelman JE, Schindlbacher A, Siciliano S, Breulmann M, Yannarell A, et al. Microbes as engines of ecosystem function: when does community structure enhance predictions of ecosystem processes? Frontiers in microbiology. 2016;7:214.

5. Martiny JB, Jones SE, Lennon JT, Martiny AC. Microbiomes in light of traits: a phylogenetic perspective. Science. 2015;350(6261).

6. Carini P, Marsden PJ, Leff JW, Morgan EE, Strickland MS, Fierer N. Relic DNA is abundant in soil and obscures estimates of soil microbial diversity. Nature microbiology. 2016;2(3):1-6.

7. Kleiner M. Metaproteomics: much more than measuring gene expression in microbial communities. Msystems. 2019;4(3):e00115-19.

8. Prosser JI. Ecosystem processes and interactions in a morass of diversity. FEMS Microbiology Ecology. 2012;81(3):507-19.

9. Schimel J, Schaeffer SM. Microbial control over carbon cycling in soil. Frontiers in microbiology. 2012;3:348.

503 10. Jansson JK, Hofmockel KS. Soil microbiomes and climate change. Nature Reviews
504 Microbiology. 2020;18(1):35-46.
505 11. Baveye PC, Otten W, Kravchenko A. elucidating microbial processes in soils and
506 sediments: microscale measurements and modeling. Frontiers in Environmental Science.
507 2019;7:78.
508 12. Jessup CM, Kassen R, Forde SE, Kerr B, Buckling A, Rainey PB, et al. Big questions,
509 small worlds: microbial model systems in ecology. Trends in ecology & evolution.
510 2004;19(4):189-97.
511 13. Prosser JI, Bohannan BJ, Curtis TP, Ellis RJ, Firestone MK, Freckleton RP, et al. The
512 role of ecological theory in microbial ecology. Nature Reviews Microbiology. 2007;5(5):384-92.
513 14. Vandevivere P, Kirchman DL. Attachment stimulates exopolysaccharide synthesis by a
514 bacterium. Applied and environmental microbiology. 1993;59(10):3280-6.
515 15. Prigent-Combaret C, Vidal O, Dorel C, Lejeune P. Abiotic surface sensing and biofilm-
516 dependent regulation of gene expression in Escherichia coli. Journal of bacteriology.
517 1999;181(19):5993-6002.
518 16. Reed SC, Cleveland CC, Townsend AR. Functional ecology of free-living nitrogen
519 fixation: a contemporary perspective. Annual review of ecology, evolution, and systematics.
520 2011;42:489-512.
521 17. Smercina DN, Evans SE, Friesen ML, Tiemann LK. To fix or not to fix: controls on free-
522 living nitrogen fixation in the rhizosphere. Applied and Environmental Microbiology.
523 2019;85(6).

524 18. Allaway D, Lodwig E, Crompton L, Wood M, Parsons R, Wheeler T, et al. Identification
525 of alanine dehydrogenase and its role in mixed secretion of ammonium and alanine by pea
526 bacteroids. Molecular microbiology. 2000;36(2):508-15.
527 19. Li Y, Parsons R, Day DA, Bergersen FJ. Reassessment of major products of N2 fixation
528 by bacteroids from soybean root nodules. Microbiology. 2002;148(6):1959-66.
529 20. Udvardi M, Poole PS. Transport and metabolism in legume-rhizobia symbioses. Annual
530 review of plant biology. 2013;64:781-805.
531 21. Waters JK, Mawhinney TP, Emerich DW. Nitrogen assimilation and transport by ex
532 planta nitrogen-fixing Bradyrhizobium diazoefficiens bacteroids is modulated by oxygen,
533 bacteroid density and L-malate. International Journal of Molecular Sciences. 2020;21(20):7542.
534 22. Setubal JC, Dos Santos P, Goldman BS, Ertesvåg H, Espin G, Rubio LM, et al. Genome
535 sequence of Azotobacter vinelandii, an obligate aerobe specialized to support diverse anaerobic
536 metabolic processes. Journal of bacteriology. 2009;191(14):4534-45.
537 23. Jeong H, Park S-Y, Chung W-H, Kim SH, Kim N, Park S-H, et al. Draft genome
538 sequence of the Paenibacillus polymyxa type strain (ATCC 842T), a plant growth-promoting
539 bacterium. Am Soc Microbiol; 2011.
540 24. Baldani JI, Reis VM, Videira SS, Boddey LH, Baldani VLD. The art of isolating
541 nitrogen-fixing bacteria from non-leguminous plants using N-free semi-solid media: a practical
542 guide for microbiologists. Plant and soil. 2014;384(1):413-31.
543 25. Nakayasu ES, Nicora CD, Sims AC, Burnum-Johnson KE, Kim Y-M, Kyle JE, et al.
544 MPLEx: a robust and universal protocol for single-sample integrative proteomic, metabolomic,
545 and lipidomic analyses. MSystems. 2016;1(3).

546 26. Rhine E, Mulvaney R, Pratt E, Sims G. Improving the Berthelot reaction for determining
547 ammonium in soil extracts and water. Soil Science Society of America Journal. 1998;62(2):473-
548 80.
549 27. Kim Y-M, Nowack S, Olsen MT, Becraft ED, Wood JM, Thiel V, et al. Diel
550 metabolomics analysis of a hot spring chlorophototrophic microbial mat leads to new hypotheses
551 of community member metabolisms. Frontiers in microbiology. 2015;6:209.
552 28. Snijders AM, Langley SA, Kim Y-M, Brislawn CJ, Noecker C, Zink EM, et al. Influence
553 of early life exposure, host genetics and diet on the mouse gut microbiome and metabolome.
554 Nature microbiology. 2016;2(2):1-8.
555 29. Kim Y-M, Schmidt BJ, Kidwai AS, Jones MB, Kaiser BLD, Brewer HM, et al.
556 Salmonella modulates metabolism during growth under conditions that induce expression of
557 virulence genes. Molecular BioSystems. 2013;9(6):1522-34.
558 30. Nagy G, Veličković D, Chu RK, Carrell AA, Weston DJ, Ibrahim YM, et al. Towards
559 resolving the spatial metabolome with unambiguous molecular annotations in complex biological
560 systems by coupling mass spectrometry imaging with structures for lossless ion manipulations.
561 Chemical Communications. 2019;55(3):306-9.
562 31. Dixon P. VEGAN, a package of R functions for community ecology. Journal of
563 Vegetation Science. 2003;14(6):927-30.
564 32. Palmer A, Phapale P, Chernyavsky I, Lavigne R, Fay D, Tarasov A, et al. FDR-
565 controlled metabolite annotation for high-resolution imaging mass spectrometry. Nature
566 methods. 2017;14(1):57-60.
567 33. Sprent JI. The biology of nitrogen-fixing organisms: McGraw-Hill Book Co.(UK) Ltd.;
568 1979.

569 34. Colnaghi R, Green A, He L, Rudnick P, Kennedy C. Strategies for increased ammonium
570 production in free-living or plant associated nitrogen fixing bacteria. Plant and Soil.
571 1997;194(1):145-54.
572 35. Ortiz-Marquez JCF, Do Nascimento M, Dublan MdlA, Curatti L. Association with an
573 ammonium-excreting bacterium allows diazotrophic culture of oil-rich eukaryotic microalgae.
574 Applied and environmental microbiology. 2012;78(7):2345-52.
575 36. Barney BM, Eberhart LJ, Ohlert JM, Knutson CM, Plunkett MH. Gene deletions
576 resulting in increased nitrogen release by Azotobacter vinelandii: application of a novel nitrogen
577 biosensor. Applied and environmental microbiology. 2015;81(13):4316-28.
578 37. Ambrosio R, Ortiz-Marquez JCF, Curatti L. Metabolic engineering of a diazotrophic
579 bacterium improves ammonium release and biofertilization of plants and microalgae. Metabolic
580 Engineering. 2017;40:59-68.
581 38. Smith MJ, Francis MB. A designed A. vinelandii–S. elongatus coculture for chemical
582 photoproduction from air, water, phosphate, and trace metals. ACS synthetic biology.
583 2016;5(9):955-61.
584 39. Ortiz-Marquez JCF, Do Nascimento M, Curatti L. Metabolic engineering of ammonium
585 release for nitrogen-fixing multispecies microbial cell-factories. Metabolic Engineering.
586 2014;23:154-64.
587 40. Wu C, Herold RA, Knoshaug EP, Wang B, Xiong W, Laurens LM. Fluxomic analysis
588 reveals central carbon metabolism adaptation for diazotroph azotobacter vinelandii ammonium
589 excretion. Scientific reports. 2019;9(1):1-11.

590 41. Vitousek PM, Cassman K, Cleveland C, Crews T, Field CB, Grimm NB, et al. Towards
591 an ecological understanding of biological nitrogen fixation. The nitrogen cycle at regional to
592 global scales: Springer; 2002. p. 1-45.
593 42. Kilstrup M, Hammer K, Ruhdal Jensen P, Martinussen J. Nucleotide metabolism and its
594 control in lactic acid bacteria. FEMS microbiology reviews. 2005;29(3):555-90.
595 43. Beaman TC, Hitchins A, Ochi K, Vasantha N, Endo T, Freese E. Specificity and control
596 of uptake of purines and other compounds in Bacillus subtilis. Journal of bacteriology.
597 1983;156(3):1107-17.
598 44. Yao C, Chou J, Wang T, Zhao H, Zhang B. Pantothenic acid, vitamin C, and biotin play
599 important roles in the growth of Lactobacillus helveticus. Frontiers in microbiology.
600 2018;9:1194.
601 45. Peterson W, Peterson MS. Relation of bacteria to vitamins and other growth factors.
602 Bacteriological reviews. 1945;9(2):49-109.
603 46. Palacios OA, Bashan Y, de-Bashan LE. Proven and potential involvement of vitamins in
604 interactions of plants with plant growth-promoting bacteria—an overview. Biology and fertility
605 of soils. 2014;50(3):415-32.
606 47. Inomura K, Bragg J, Follows MJ. A quantitative analysis of the direct and indirect costs
607 of nitrogen fixation: a model based on Azotobacter vinelandii. The ISME journal.
608 2017;11(1):166-75.
609 48. Dixon R, Kahn D. Genetic regulation of biological nitrogen fixation. Nature Reviews
610 Microbiology. 2004;2(8):621-31.

611 49. Gonzalez-Lopez J, Salmeron V, Moreno J, Ramos-Cormenzana A. Amino acids and
612 vitamins produced by Azotobacter vinelandii ATCC 12837 in chemically-defined media and
613 dialysed soil media. Soil Biology and Biochemistry. 1983;15(6):711-3.
614 50. Martinez-Toledo MV, Rodelas B, Salmeron V, Pozo C, Gonzalez-Lopez J. Production of
615 pantothenic acid and thiamine by Azotobacter vinelandii in a chemically defined medium and a
616 dialysed soil medium. Biology and fertility of soils. 1996;22(1):131-5.
617 51. Danczak RE, Chu RK, Fansler SJ, Goldman AE, Graham EB, Tfaily MM, et al. Using
618 metacommunity ecology to understand environmental metabolomes. Nature communications.
619 2020;11(1):1-16.
620 52. Danczak RE, Goldman AE, Chu RK, Toyoda JG, Garayburu-Caruso VA, Tolić N, et al.
621 Ecological theory applied to environmental metabolomes reveals compositional divergence
622 despite conserved molecular properties. Science of The Total Environment. 2021;788:147409.
623 53. Wilson RM, Tfaily MM, Kolton M, Johnston ER, Petro C, Zalman CA, et al. Soil
624 metabolome response to whole-ecosystem warming at the Spruce and Peatland Responses under
625 Changing Environments experiment. Proceedings of the National Academy of Sciences.
626 2021;118(25).
627 54. Song Y, Li X, Yao S, Yang X, Jiang X. Correlations between soil metabolomics and
628 bacterial community structures in the pepper rhizosphere under plastic greenhouse cultivation.
629 Science of The Total Environment. 2020;728:138439.
630 55. Boddy E, Hill PW, Farrar J, Jones DL. Fast turnover of low molecular weight
631 components of the dissolved organic carbon pool of temperate grassland field soils. Soil Biology
632 and Biochemistry. 2007;39(4):827-35.

633 56. Hill PW, Farrar JF, Jones DL. Decoupling of microbial glucose uptake and
634 mineralization in soil. Soil Biology and Biochemistry. 2008;40(3):616-24.
635 57. Pétriacq P, Williams A, Cotton A, McFarlane AE, Rolfe SA, Ton J. Metabolite profiling
636 of non-sterile rhizosphere soil. The Plant Journal. 2017;92(1):147-62.
637 58. Swenson TL, Jenkins S, Bowen BP, Northen TR. Untargeted soil metabolomics methods
638 for analysis of extractable organic matter. Soil Biology and Biochemistry. 2015;80:189-98.
639 59. Dungait JA, Hopkins DW, Gregory AS, Whitmore AP. Soil organic matter turnover is
640 governed by accessibility not recalcitrance. Global Change Biology. 2012;18(6):1781-96.
641 60. Wilkinson A, Hill PW, Farrar JF, Jones DL, Bardgett RD. Rapid microbial uptake and
642 mineralization of amino acids and peptides along a grassland productivity gradient. Soil Biology
643 and Biochemistry. 2014;72:75-83.
644 61. Hobbie JE, Hobbie EA. Amino acid cycling in plankton and soil microbes studied with
645 radioisotopes: measured amino acids in soil do not reflect bioavailability. Biogeochemistry.
646 2012;107(1):339-60.
647 62. Drescher K, Nadell CD, Stone HA, Wingreen NS, Bassler BL. Solutions to the public
648 goods dilemma in bacterial biofilms. Current Biology. 2014;24(1):50-5.
649 63. Stewart PS. Diffusion in biofilms. Journal of bacteriology. 2003;185(5):1485-91.
650 64. Flemming H-C, Wingender J. The biofilm matrix. Nature reviews microbiology.
651 2010;8(9):623-33.
652 65. Wang D, Xu A, Elmerich C, Ma LZ. Biofilm formation enables free-living nitrogen-
653 fixing rhizobacteria to fix nitrogen under aerobic conditions. The ISME journal.
654 2017;11(7):1602-13.

655 66. Rinaudi L, Fujishige NA, Hirsch AM, Banchio E, Zorreguieta A, Giordano W. Effects of
656 nutritional and environmental conditions on Sinorhizobium meliloti biofilm formation. Research
657 in microbiology. 2006;157(9):867-75.
658 67. Jung J-H, Choi N-Y, Lee S-Y. Biofilm formation and exopolysaccharide (EPS)
659 production by Cronobacter sakazakii depending on environmental conditions. Food
660 microbiology. 2013;34(1):70-80.
661
662
663
664
665
666
667
668
669
670
671
672
673
674
675
676
677

678 **Figure legends**

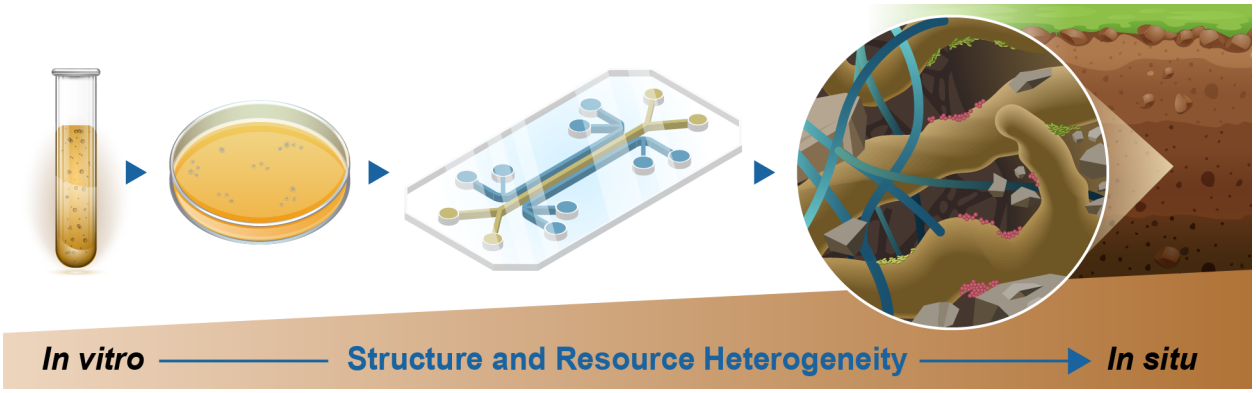

679

680 **Fig. 1**: Depiction of the systematic scaling of system complexity from liquid and solid culture to

681 synthetic soils (represented here as a microfluidic chip) to *in situ* soil conditions. In our study we

682 focus on the first two steps, relating metabolomics in liquid and solid media culture.

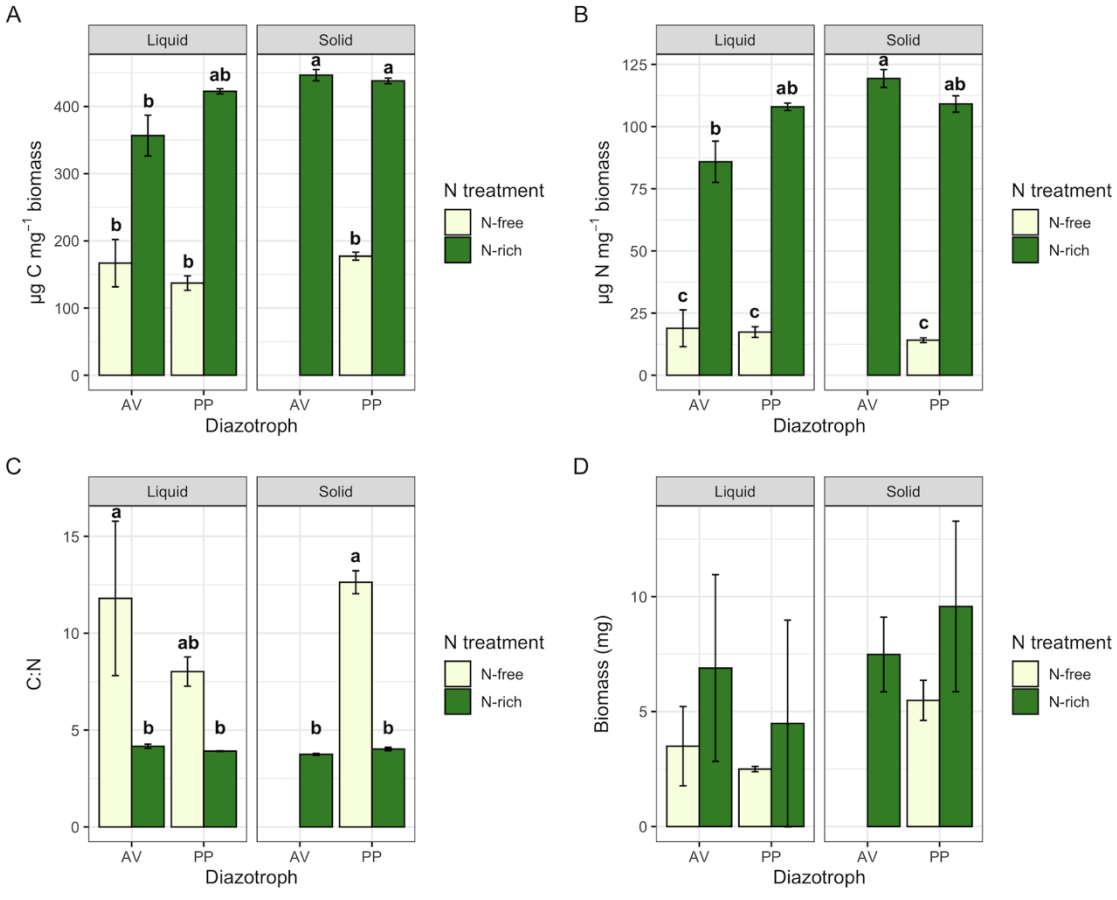

683

684 **Fig. 2:** Microbial (A) C content, (B) N content, (C) C:N ratio, and (D) total biomass. Bars
685 represent average values ± standard error and are colored by nitrogen treatment. Figures are
686 faceted by culture type. Lowercase letters represent significant difference at $p < 0.05$.

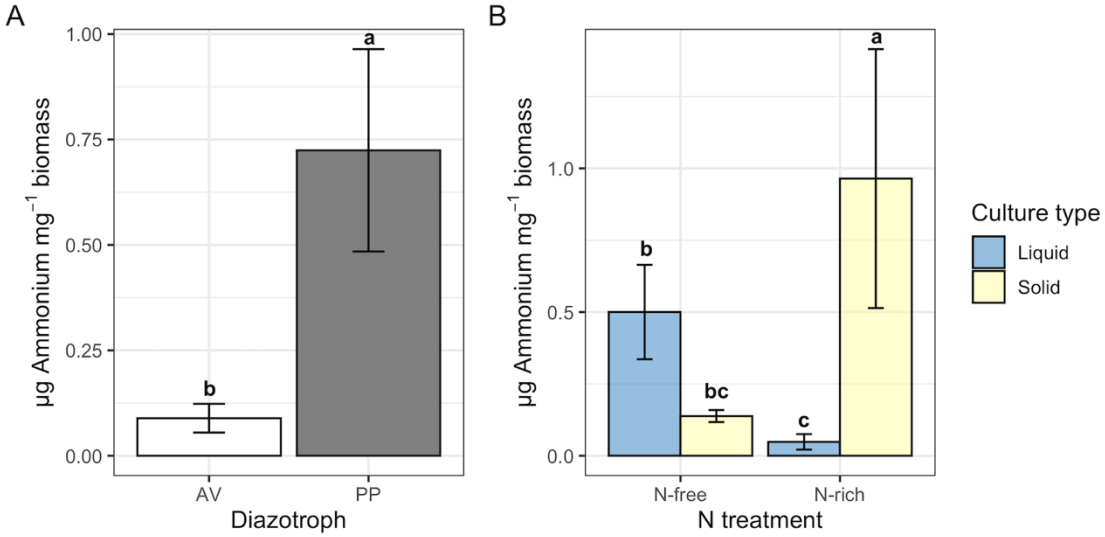

687

688 **Fig. 3:** Extracellular ammonium availability per unit biomass shown by (A) diazotrophic
689 organism and by (B) N treatment. Bars represent average values ± standard error. Bars in (B) are
690 colored by culture type. Lowercase letters indicate significant difference at $p < 0.05$.

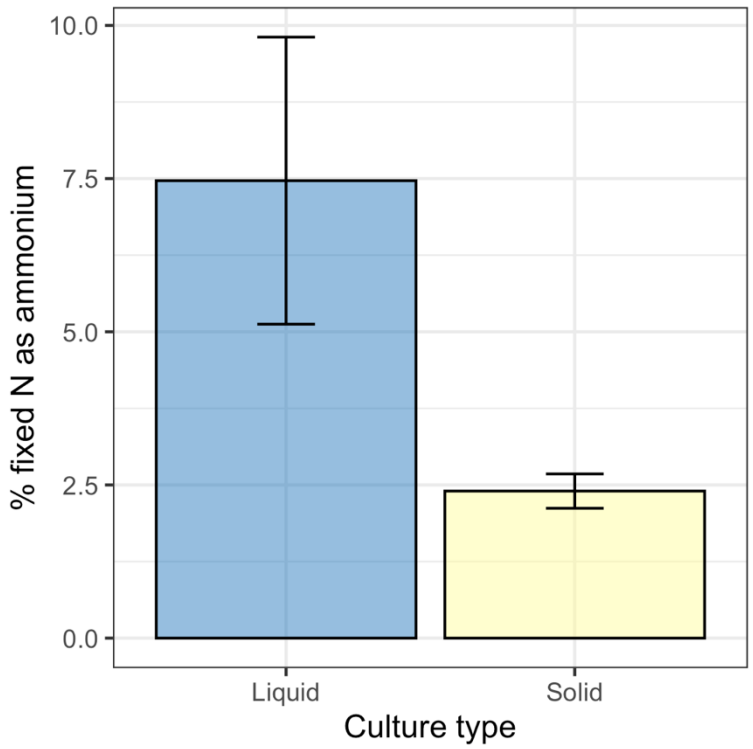

Fig. 4: Percent of fixed nitrogen available as extracellular ammonium in N-free treatments. Bars represent average ± standard error. No significant difference was observed between culture types.

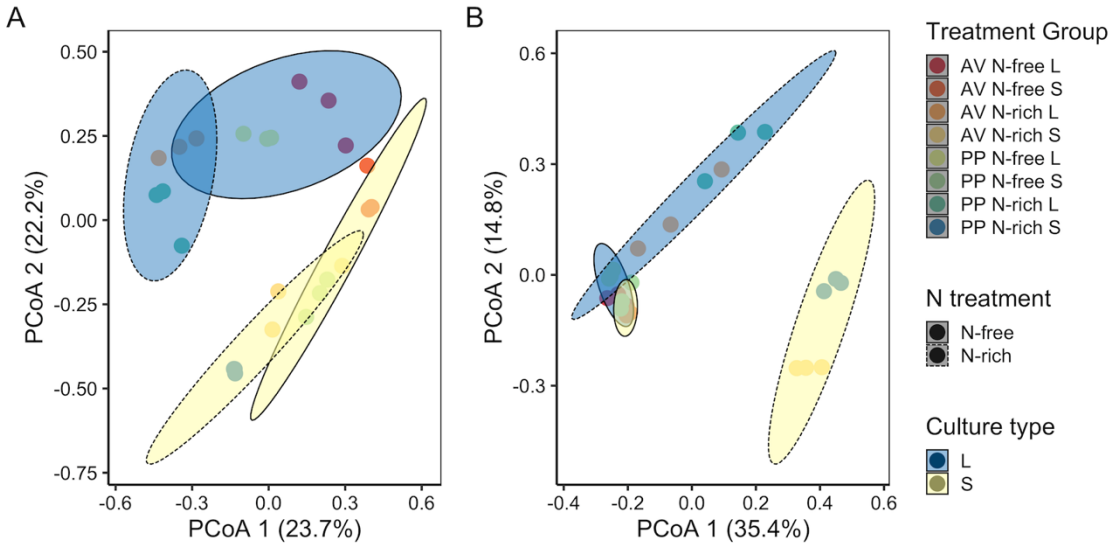

696 **Fig. 5:** Principal coordinates analysis (PCoA) of metabolite chemistry based on (A) Bray-Curtis
697 of peak intensity and (B) Jaccard of presence-absence including all detected metabolites. Each
698 point represents a single sample and are colored by treatment group (organism, N treatment,
699 culture type). 95% confidence ellipses are shown for culture type, represented by color, and N
700 treatment, represented by line type.

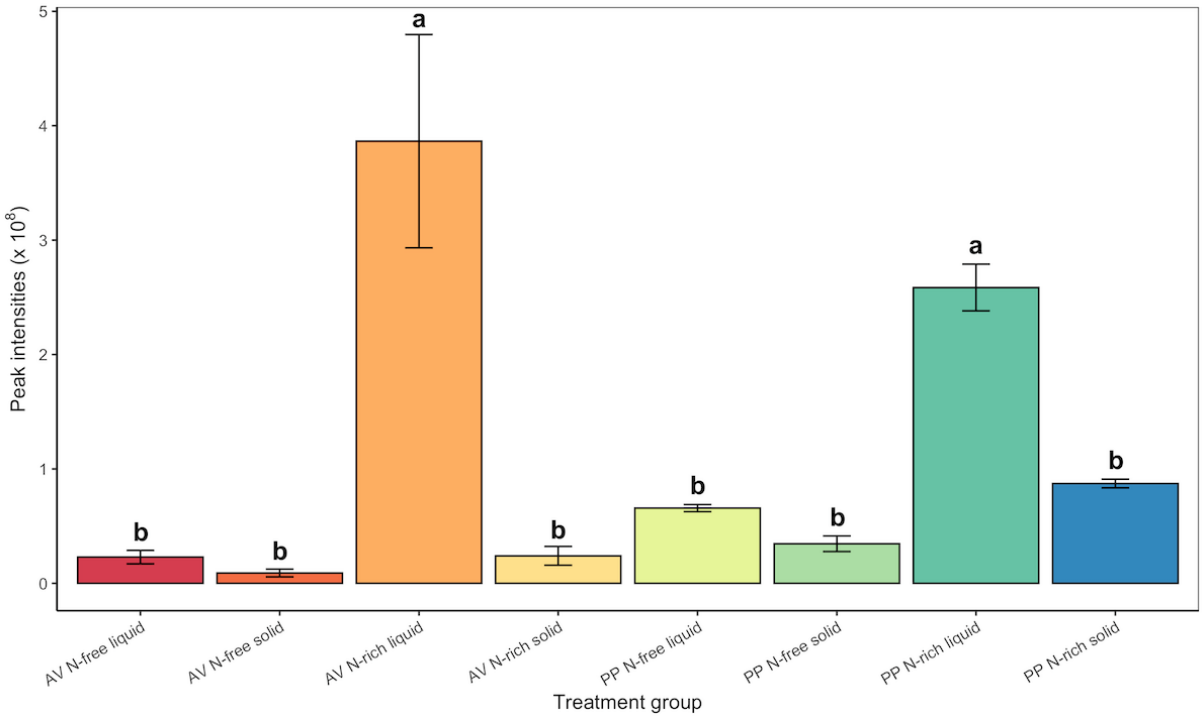

701

702 **Fig. 6:** Peak intensities of N-containing metabolites detected across treatment groups. Bars
703 represent average peak intensity ± standard error. Lowercase letters indicate significant
704 difference at $p < 0.05$.

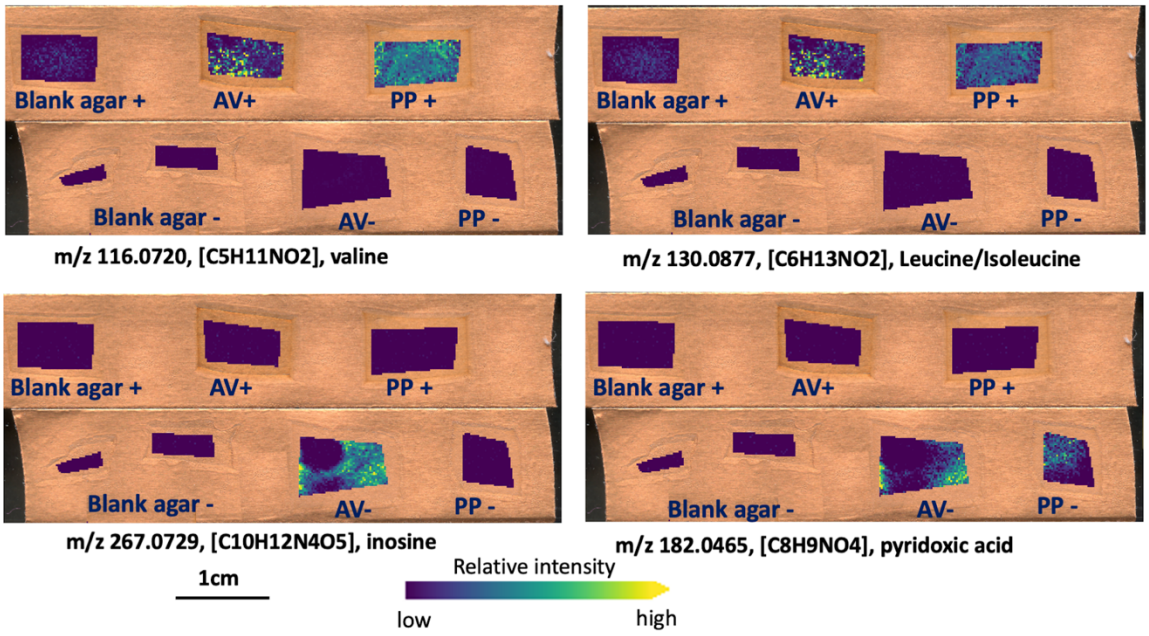

705

706 **Fig. 7:** Examples of the N-containing metabolites detected at the microscale using MALDI MSI.

707 All ions are annotated as [M–H]- adducts. Ion images of individual m/z values were generated on

708 the same color bar scale for visual comparison in terms of relative ion abundance.

709

Table 1: PERMANOVA results for Bray-Curtis and Jaccard distance of macroscale metabolite abundance.

		Df	Sums of Squares	Mean Squares	F model	R squared	p–value
Bray-Curtis	N treatment	1	1.422	1.422	7.899	0.192	0.0001
	Culture type	1	1.548	1.548	8.599	0.209	0.0001
	Interaction	1	0.841	0.842	4.676	0.114	0.0001
	Residual	20	3.601	0.180		0.486	
	Total	23	7.413			1	
Jaccard	N treatment	1	1.350	1.350	11.547	0.279	0.0001
	Culture type	1	0.639	0.639	5.460	0.132	0.0003
	Interaction	1	0.515	0.515	4.406	0.106	0.0016
	Residual	20	2.339	0.117		0.483	
	Total	23	4.843			1	

710